Applied Energy 268 (2020) 114952

Contents lists available at ScienceDirect

Applied Energy

journal homepage: www.elsevier.com/locate/apenergy

Performance analysis of metaheuristic optimization algorithms in estimating the parameters of several wind speed distributions

Kevin S. Guedes[a,*], Carla F. de Andrade[a], Paulo A.C. Rocha[a], Rivanilso dos S. Mangueira[a], Elineudo P. de Moura[b]

[a] Mechanical Engineering Department, Technology Center, Federal University of Ceará, Fortaleza, CE 60020-181, Brazil
[b] Department of Metallurgical and Materials Engineering, Technology Center, Federal University of Ceará, Fortaleza, CE 60020-181, Brazil

HIGHLIGHTS

- 11 distributions are used to fit the wind speed data of two Brazilian regions.
- The application of optimization methods is expanded to non-conventional distributions.
- The coefficient of determination as objective function yielded better results.
- Metaheuristic optimization algorithms outperformed Maximum Likelihood method.
- Gamma Generalized and Extended Generalized Lindley distributions fitted better.

ARTICLE INFO

Keywords:
Wind energy
Wind speed modeling
Optimal parameters estimation
Multi-criteria statistical analysis
Metaheuristic optimization algorithms
Non-conventional wind speed distributions

ABSTRACT

For a better use of wind energy, the accurate selection of the wind speed distributions that best represents the regarding wind regime's characteristics is essential. The Weibull distribution is the most common, but this model is not always the most suitable. Therefore, in order to obtain more reliable information, the evaluation of different distributions becomes necessary. Another crucial step is the estimation of the parameters that govern these distributions because the accuracy of these estimates directly affects the energy generation calculations. In the last few years, different optimization methods have been used for this purpose. However, the applications of these methods are focused on conventional two-parameter distributions, such as Weibull and Lognormal. Futhermore, different authors report that there is a lack of studies that use optimization methods for this purpose. In this paper, four metaheuristic optimization algorithms (MOA)—namely, Migrating Birds Optimization (MBO), Imperialist Competitive Algorithm (ICA), Harmony Search (HS) and Cuckoo Search (CS)—are used to fit 11 distributions in two Brazillian regions. Thus, this work expands the application of the MOA to beyond the conventional distributions and applies, for the first time, the MBO and ICA in estimating the parameters of wind speed distributions, thereby introducing new ways to optimize the use of wind resources. The fits obtained by the MOA were compared with those obtained by the method Maximum Likelihood Estimation (MLE). Gamma Generalized and Extended Generalized Lindley distributions presented the best fits, and the MOA outperformed the MLE because the global score values obtained were smaller.

1. Introduction

Amid growing demand for energy and the environmental impacts caused by the use of fossil fuels, renewable sources have received special attention as viable means of supplying this need and reducing carbon dioxide emissions into the atmosphere and dependence on fossil fuels. Among the various renewable sources, wind energy has experienced the fastest development rate in many regions of the planet. For the efficient use of wind resources in a region, the knowledge of the wind regime characteristics is of paramount importance [1]. Among the many factors that affect the output power of a wind turbine, wind speed distribution is the most important [2]. If this distribution is known, then the wind potential and the economic viability of the wind farm can be easily calculated [3]. These distributions are also used in wind farm

* Corresponding author.
E-mail addresses: kevin_guedes@hotmail.com (K.S. Guedes), carla@ufc.br (C.F. de Andrade), paulo.rocha@ufc.br (P.A.C. Rocha), elineudo@ufc.br (E.P. de Moura).

https://doi.org/10.1016/j.apenergy.2020.114952
Received 24 October 2019; Received in revised form 25 March 2020; Accepted 2 April 2020
Available online 07 May 2020
0306-2619/

Nomenclature

Symbols

x	Wind speed data
$\bar{x}$	Mean of the wind speed data
s	Standard deviation of the wind speed data
k	Shape parameter
c	Scale parameter
p	Second shape parameter
u	Location parameter
n	Total number of data points
$f(x)$	Probability density function
$F(x)$	Cumulative distribution function
$\overline{P}_w$	Average wind turbine power output
$P_w(x)$	Wind turbine power output as function of the wind speed
R^2	Coefficient of determination
F_i	Observed cumulative probabilities
$\hat{F}_i$	Predicted cumulative probabilities
γ_u	Upper incomplete gamma function
γ_l	Lower incomplete gamma function
Φ	Standard normal cumulative distribution function
erf	Error function
N_{birds}	Number of birds in the V formation
n_{nb}	Number of neighboring solutions
n_{un}	Number of unused solutions
b	Bird (solution)
$\hat{b}$	Neighboring solution
m	Number of iterations for shifting the leader bird
$n_{[i,j]}$	Random number ranging from i to j
$N_{countries}$	Number of countries
N_{imp}	Number of imperialists
N_{col}	Number of colonies
TC_i	Total cost of the ith empire
NTC_i	Normalized TC_i
P_{p_i}	Possession probability of the ith empire
N_h	Number of harmonies
bw	Bandwidth
N_{nests}	Number of birds in the V formation
p_d	Probability of a cuckoo egg being detected
$Lévy(\lambda)$	Lévy distribution
α	Constant in cuckoo search algorithm
$\oplus$	Entrywise multiplications
L	Likelihood function
n_p	Number of parameters
g_1	Empirical skewness
g_2	Empirical kurtosis
γ_1	Theoretical skewness
γ_2	Theoretical kurtosis
w_{ij}	ith value of the j criterion
$\bar{w}_j$	Mean of of the j criterion
s_j	Standard deviation of the j criterion
z_{ij}	Standardized score

Abbreviations

W	Weibull
G	Gamma
BS	Birnbaum-Saunders
N	Nakagami
LN	Lognormal
GL	Generalized Lindley
GEV	Generalized Extreme Value
B	Burr
D	Dagum
EGL	Extended generalized lindley
GG	Generalized gamma
R	Rayleigh
LL	Loglogistic
Norm	Normal
RMSE	Root mean square error
NRMSE	Normalized *RMSE*
SCR-25	Station in São João do Cariri
PTR-11	Station in Petrolina
MOA	Metaheuristic optimization algorithms
MBO	Migrating birds optimization
ICA	Imperialist competitive algorithm
HS	Harmony Search
CS	Cuckoo Search
PSO	Particle swarm optimization
ACA	Ant colony algorithm
MLE	Maximum likelihood estimation
MMLE	Modified MLE
MM	Method of moments
LSM	Least squares method
EM	Empirical method
EPF	Energy pattern factor method
GM	Graphical method
NM	Numerical methods
SONDA	Sistema de Organização Nacional de Dados Ambientais (National Organization System of Environmental Data)
HMCR	Harmony Memory Considering Rate
PAR	Pitch adjusting rate
AIC	Akaike information criterion
DSK	Deviation of skewness and kurtosis
KS	Kolgomorov-Smirnov test
SNCDFT	Standard normal cumulative distribution function transformation
GS	Global Score

planning; in the calculation of important indicators such as average wind power density, effective wind power density, availability factor and capacity factor; and to reduce uncertainties linked to wind potential development [4,5].

The Weibull (W) distribution is one of the most widely used. The ease of estimating the two parameters of this distribution, its flexibility and its good accuracy in different regions are some of the main features that make this distribution one of the most used [3]. However, this distribution is not always the most suitable to describe certain wind regimes [4].

Soukissian [6] also state that the Weibull distribution has been often proved to be inadequate and its indiscriminate use is not justified. Amid this scenario, the authors proposed, for the first time, the use of the Johnson S_B distribution for offshore wind speed modeling. The results showed that the Johnson S_B distribution accurately describes the empirical distribution of offshore wind speed and that it has better adaptability than the 3-parameter Weibull distribution. Zhang et al. [7] applied the Maximum Entropy Principle to fit the annual wind speed data collected at Rudong, in East China Sea. The Maximum Entropy Principle performed adequately in fitting the wind speed frequency distribution when compared to the W distribution.

In a study conducted by Masseran [8] with data collected at two stations in Malaysia, the Gamma (G) distribution proved to be better than the traditional W to fit the wind speed data. Wang et al. [9] also affirm that the W distribution is not always able to represent some wind regimes. Kantar et al. [10] compared the performance of Extended

Generalized Lindley (EGL) distribution with that of W, Rayleigh (R), Lognormal (LN) and G distributions in different regions of Turkey. Their results show that the EGL presented the best accuracy in most of the examined regions. Similar studies have been conducted by Mohammadi et al. [5], Alavi et al. [11] and Arslan et al. [12], demonstrating the good performance, respectively, of the Birnbaum-Saunders (BS), Nakagami (N) and Generalized Lindley (GL) distributions when fitting the wind speed data of different regions. To reduce uncertainties linked to wind resource estimates, Aries et al. [1] analyzed the accuracy of eight probability distributions in the modeling of wind speed in four regions of Algeria. According to their statistical tests, Coefficient of Determination and Root Mean Square Error, Gamma (G) and Generalized Extreme Value (GEV) distributions performed better. In a study conducted by Brano et al. [13] in southern Italy, the three-parameter distribution Burr was found to be the most accurate when compared to the W, R, G, LN, Inverse Gaussian and Pearson Type V distributions. Jung and Schindler [14] evaluated the performance of 24 one-component distribution models and 24 mixed-distribution models in a study conducted on a global scale and from the results it was shown that only in a few regions did the W distribution provide the highest accuracy. Given these facts, it is possible to see that the accuracy of a distribution is directly related to the characteristics of the wind regime in which it was applied, such that if a given distribution model showed good accuracy in a region, then this does not mean that it will provide a good fit in all regions. Thus, to obtain a more accurate fit, it is essential to analyze different distribution models.

Another very important step is the correct estimation of the parameters governing the probability distribution functions. Although a given distribution can accurately represent the wind regime of a region, if its parameters are not estimated correctly, then the fit obtained will be inaccurate and unreliable. The analysis of the wind potential of a region and the economic viability of a project are important aspects that depend on the good estimation of these parameters [15]. Consequently, to obtain a more accurate fit, most researchers use several methods of parameter estimation. The most commonly used methods are: Maximum Likelihood Estimation (MLE) [16], Modified Maximum Likelihood Estimation (MMLE) [17], Graphical Method (GM) [18], Method of Moments (MM) [19,1], Least Squares Method (LSM) [14,20], Empirical Method (EM) [21] and Energy Pattern Factor Method (EPF) [22]. Such methods are classified as Numerical Methods (NM). However, there is another category, composed by Metaheuristic Optimization Algorithms (MOA), whose application in the optimization of the distributions unknown parameters has proven to be beneficial and promising. In addition, many studies have shown the superior performance of these methods when compared to the traditional NM.

Wang et al. [4] used the Particle Swarm Optimization (PSO), Cuckoo Search (CS) and Gray Wolf Optimizer optimization methods and the EM, EPF, and MLE numerical methods to estimate the W distribution parameters in China. Their statistical analysis demonstrated that the fits obtained by optimization methods were usually superior to the fits obtained by numerical methods. Jiang et al. [19] estimated the parameters of the W, R, G and LN distributions through the optimization methods PSO, CS and Bat Algorithm and the numerical methods MM, MLE and LSM. Subsequently, a comparative analysis was conducted and the results showed that all the optimization methods performed better than the numerical methods. Wang et al. [23] used Chaotic PSO and CS to estimate the parameters of the GEV and Gumbel distributions in offshore extreme wind speed modeling. Both methods presented a good performance. Wang et al. [9] used the CS to fit the W, G, R, LN, Normal (Norm), and Loglogistic (LL) distributions in four regions of China. Their study revealed that the CS algorithm outperformed the widely used estimation methods. Similarly, Zhao et al. [3] and Wang et al. [24] used the CS, Ant Colony Algorithm (ACA), Genetic Algorithm and Firefly Algorithm to calculate the parameters of the W distribution. Andrade et al. [25] did the same using the optimization methods Harmony Search (HS), PSO, CS and ACA. Chang [26] and Wu et al. [27] used the PSO to estimate the unknown parameters in the W distribution.

However, from this literature review, it is possible to observe that the optimization methods were mostly employed in more commonly used two-parameter distributions (i.e., W, G, LN, Norm and LL). In addition, according to Jiang et al. [19], previous studies and applications of optimization methods to estimate wind speed distribution parameters are insufficient. Furthermore, Wang et al. [4] highlighted the lack of studies using optimization methods to estimate the W distribution parameters.

In this paper, inspired by the scenarios presented above, six two-parameters distributions—namely Weibull (W), Gamma (G), Birnbaum-Saunders (BS), Nakagami (N), Lognormal (LN) and Generalized Lindley (GL)—and five three-parameter distributions—namely Generalized Extreme Value (GEV), Burr (B), Dagum (D), Extended Generalized Lindley (EGL), and Generalized Gamma (GG)—were used to fit the wind speed data of two cities in northeastern Brazil. The optimal parameters of these distributions were estimated through four MOA—namely, Migrating Birds Optimization (MBO), Imperialist Competitive Algorithm (ICA), Harmony Search (HS) and Cuckoo Search (CS). Regarding the MBO and ICA methods, no studies were found in the literature that used these methods to fit wind speed distributions. Consequently, this paper is the first time that these methods have been applied for this purpose. Regarding HS, no studies were found that analyzed its performance when fitting three-parameter distributions.

The results provided by the MOA are compared with the results obtained by the deterministic method Maximum Likelihood Estimation (MLE) through an integrated approach recently proposed by Masseran [8] that considers mutually, in a single value, four statistical tests that are commonly used in this type of study—namely, Coefficient of Determination (R^2), Kolgomorov-Smirnov Test (*KS*), Akaike Information Criterion (*AIC*) and Deviation of Skewness and Kurtosis (*DSK*)—to evaluate the performance and applicability of the MBO and ICA methods in the estimation of the wind speed distribution parameters, of the HS method in fitting the three-parameter distributions, and to determine the sets (distribution - parameters estimation method) that provide a better fit.

This paper presents a new application of the MBO, ICA and HS methods. This is the first time that MBO and ICA have been used to determine the optimal parameters of wind speed distributions, thereby introducing new ways to optimize the use of wind resources. This also expands the application of MOA to beyond the conventional two-parameter distributions, which until now were the application focus of these methods. As mentioned before, in the studies conducted by Wang et al. [4], Zhao et al. [3], Wang et al. [24,9], Jiang et al. [19], Chang [26], Andrade et al. [25] and Wu et al. [27], for example, the optimization methods were all applied to estimate the unknown parameters of two-parameter distributions.

This paper also compares the performance of the MOA with three distinct objective functions to determine which one provides the greater accuracy when fitting the distributions, it also presents a broad and objective comparison of the accuracy of a specific group of eleven wind speed distributions fitted through four MOA. Eight non-conventional distributions (BS, N, GL, GEV, B, D, EGL and GG) and three conventional (W, G and LN) are included in this group.

2. Wind speed data and site presentation

In this research, the wind speed data used were obtained at PTR-11 station, located in the city of Petrolina, and at SCR-25 station, located in the city of São João do Cariri, both in the northeast region of Brazil. The data were provided by the Sistema de Organização Nacional de Dados Ambientais (SONDA - National Organization System of Environmental Data), which is a project of the Brazilian Federal Government. Geographic information of both regions are presented in Table 1.

The Northeast of Brazil is one of the best regions in the world for

Table 1
Geographical information (Latitude, Longitude and Altitude) of PTR-11 and SCR-25 stations.

Site	Latitude (°)	Longitude (°)	Altitude (m)
São João do Cariri (Station SCR-25)	−7.3817	−36.5272	718
Petrolina (Station PTR-11)	−9.0689	−40.3197	387

wind power generation thanks to the extremely favorable characteristics of the wind regime. Consequently, 86% of Brazil's installed wind power capacity is located in the Northeast region. According to the Associação Brasileira de Energia Eólica (Brazilian Wind Energy Association) [28], during the "harvest of the wind" season, which corresponds to the months of June to November, it is common for wind farms in the Brazilian Northeast to reach capacity factors greater than 80%, which is a significantly higher value than the world average of approximately 25%. During this same period in 2018, wind energy supplied 104% of the region's demand, with surplus energy being exported to other regions of the country. These facts, coupled with the enormous potential that is still unexplored in this region, justify the choice of the wind speed data from the cities of São João do Cariri and Petrolina and they highlight the importance of this study for the development of the wind potential in the Northeast of Brazil.

Before being made available, the wind speed data are subjected to a validation process based on Baseline Surface Radiation Network data quality control. This process does not correct the data but it does generate a validation code that signals the data characterized as suspicious, it is at the discretion of the user to use it or not. On the selected data, only a small percentage was characterized as suspect.

Faced with this situation, the data were subjected to a treatment process to remove suspicious values (i.e., non-numeric, negative and excessive values). In both regions, the percentage of utilization was higher than 99%, which demonstrates the high reliability of the data. Table 2 presents some basic information about the data collected by stations SCR-25 and PTR-11. The average wind speeds of both were measured in m/s every 10 min, at 50 m height, for one year. The time history of wind speed and the "harvest of the wind" season for both stations are presented in Fig. 1.

3. Wind speed distribution models

In mathematical terms, the average wind turbine power output $\overline{P_w}$ is given by [14]:

$$\overline{P_w} = \int_0^\infty P_w(x) f(x) dx \tag{1}$$

where $P_w(x)$ is the wind turbine power output as a function of the wind speed x and $f(x)$ is a probability distribution function. From Eq. (1), it is easy to see that the incorrect selection of the most accurate $f(x)$ function and/or a poor parameter estimation of this distribution directly impacts the average power generated by the wind turbine, which may compromise the wind resource analysis and the energy generation efficiency in a given region. Garrido-Perez et al. [29], for example, used the Weibull distribution to identify regional differences in the sites analyzed in their study and to estimate the expected wind production. Sedaghat et al. [30] introduced a capacity value, which represents the annual wind energy production from a specific wind site using a certain wind turbine. This capacity value is calculated in terms of the Weibull distribution and power performance of variable wind speed turbines. These studies highlight the importance and the application of an accurate wind speed distribution model in analysing the wind resources. These studies are based in the Weibull distribution, but as stated by different author, this model is not always the most suitable.

Therefore, to ensure the selection of an accurate model, 11 probability distributions were evaluated in this research, as follows: Weibull (W), which is one of the most widely used in wind resource modeling and presents good performance in several regions; Gamma (G) and Lognormal (LN), which are both also very common in wind resource analysis; Birnbaum-Saunders (BS), Nakagami (N), Generalized Lindley (GL) and Extended Generalized Lindley (EGL) models, whose application in wind energy is more recent; Burr (B), Dagum (D), Generalized Extreme Value (GEV) and Generalized Gamma (GG), which are more flexible models and presented high performance in different regions.

The W, G, BS, N, LN and GL models have two parameters and the GEV, B, D, EGL and GG models have three parameters. The probability density function $f(x)$ and the cumulative distribution function $F(x)$ of these models are presented in Table 3, where k is the shape parameter, p is the second shape parameter, c is the scale parameter and u is the location parameter.

4. Parameter optimization methods

The estimation and the optimization of unknown distributions parameters is crucial to select the most suitable probability model [19]. In this study, four metaheuristic optimization algorithms (MOA) were used—namely, Migrating Birds Optimization (MBO), Imperialist Competitive Algorithm (ICA), Harmony Search (HS) and Cuckoo Search (CS)—to determine optimal parameters and provide a more accurate fit.

These methods have been selected due to their proven and recent performance in various scientific fields, such as nuclear energy [41], spatial prediction of wildfire probability [42], robotics [43], image compression [44], optimization of laminated composite structures [45], structural damage detection [46], structural and design optimization [47], among others. In the case of MBO and ICA, no studies were found that used these methods to determine the optimal parameters of the wind speed distributions. Thus, the application of these methods is performed for the first time in this research. As for HS, its applications were found only in the estimation of the W distribution parameters. Finally, because according to Jiang et al. [19], only few studies have been conducted to optimize the distribution parameters through MOA. Thus, by selecting four MOA, this paper presents, as one more contribution, a broad comparison of the MOA performance in determining the optimal parameters of wind speed distributions, focusing not on a small group of conventional models but on a broad group consisting of 11 distributions, most of which are non-conventional models.

MOA methods present in their structure a certain *tradeoff* between randomness and local search. In addition, the main components of any MOA are diversification and intensification (or exploration and exploitation). Diversification is the ability of the method to generate diverse and distinct solutions, which ensures a global search in the space of possible solutions to the problem. In contrast, intensification is the ability to focus on a particular region of the search space by exploiting the information that the current best solution lies in this region. The combination of these two components generally ensures that the global optimum is achievable [48].

MOAs have an important information sharing-mechanism, which under certain circumstances can accelerate the convergence of the algorithm [49]. This sharing-mechanism is also one of the key features

Table 2
Basic statistics, size and year of measurement of the wind speed data collected in São João do Cariri (Station SCR-25) and Petrolina (Station PTR-11).

Station	SCR-25	PTR-11
Year	2008	2010
Min (m/s)	0.002	0.008
Max (m/s)	12.98	14.30
Mean (m/s)	5.238	4.886
Standard deviation (m/s)	2.332	1.745
Skewness	0.178	0.073
Kurtosis	2.449	3.105
Size	52662	52514

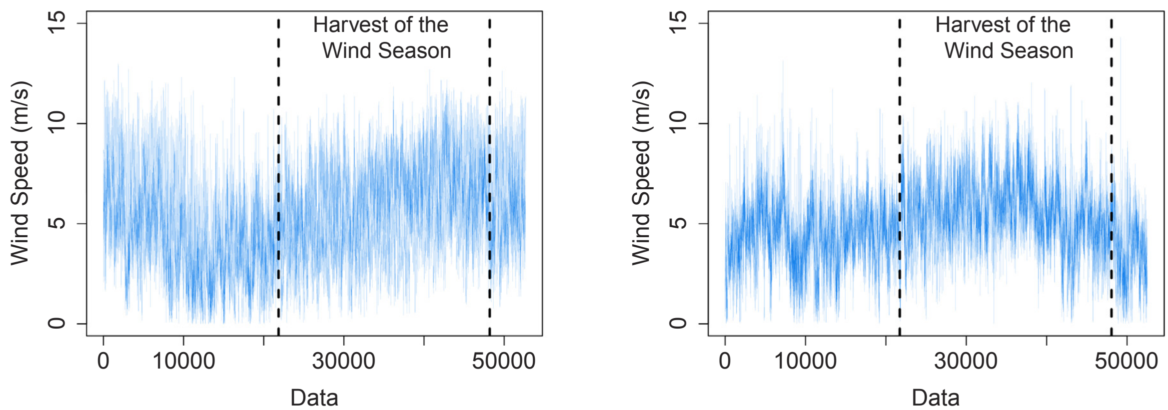

(a) Time History of Wind Speed of SCR-25 (b) Time History of Wind Speed of PTR-11

Fig. 1. Time History of Wind Speed (m/s) in a 10 min interval between each measurement. The “Harvest of the Wind” season in both regions is also displayed.

Table 3
Probability Density Function $f(x)$ and Cumulative Distribution Function $F(x)$ of each distribution model used in this work, where k is the shape parameter, p is the second shape parameter, c is the scale parameter, u is the location parameter, γ_u and γ_l are, respectively, the upper and lower incomplete gamma function, Φ is the standard normal cumulative distribution function, and *erf* is the error function. Previous studies where these distributions were used are also presented.

Model	$f(x)$	$F(x)$	References
W	$\frac{k}{c}\left(\frac{x}{c}\right)^{k-1}e^{-\left(\frac{x}{c}\right)^k}$	$1-e^{-\left(\frac{x}{c}\right)^k}$	Wang et al. [4] Jiang et al. [19] Andrade et al. [17] Usta et al. [22]
G	$\frac{x^{k-1}e^{-\frac{x}{c}}}{c^k\Gamma(k)}$	$\frac{\gamma_l\left(k,\frac{x}{c}\right)}{\Gamma(k)}$	Masseran [8] Carta et al. [16] Mazzeo et al. [31]
BS	$\frac{e^{-\frac{1}{2k^2}\left(\frac{x}{c}+\frac{c}{x}-2\right)}}{2\sqrt{2\pi}kc}\left[\left(\frac{c}{x}\right)^{\frac{1}{2}}+\left(\frac{c}{x}\right)^{\frac{3}{2}}\right]$	$\Phi\left[\frac{1}{k}\left\{\left(\frac{x}{c}\right)^{\frac{1}{2}}-\left(\frac{c}{x}\right)^{\frac{1}{2}}\right\}\right]$	Mohammadi et al. [5] Soukissian and Karathanasi [32] Miao et al. [33]
N	$\frac{2k^k}{\Gamma(k)c^k}x^{2k-1}e^{\left(-\frac{k}{c}x^2\right)}$	$1-\frac{\gamma_u\left(k,\frac{k}{c}x^2\right)}{\Gamma(k)}$	Aries et al. [1] Alavi et al. [11] Soukissian and Karathanasi [32]
LN	$\frac{1}{xk\sqrt{2\pi}}e^{\left[-\frac{1}{2}\left(\frac{ln(x)-c}{k}\right)^2\right]}$	$\frac{1}{2}+\frac{1}{2}erf\left[\frac{ln(x)-c}{k\sqrt{2}}\right]$	Aries et al. [34] Alavi et al. [35] Soukissian and Karathanasi [36]
GL	$\frac{kc^2(1+x)e^{-cx}}{c+1}\left(1-\frac{1+c+cx}{1+c}e^{-cx}\right)^{k-1}$	$\left(1-\frac{1+c+cx}{1+c}e^{-cx}\right)^k$	Arslan et al. [12]
GEV	$\frac{\left[1-\frac{k(x-u)}{c}\right]^{\frac{1}{k}-1}}{c}e^{\left[-\left(1-\frac{k(x-u)}{c}\right)^{\frac{1}{k}}\right]}$	$e^{\left[-\left(1-\frac{k(x-u)}{c}\right)^{\frac{1}{k}}\right]}$	Aries et al. [1] Mohammadi et al. [5] Miao et al. [33] Soukissian and Karathanasi [32]
B	$\frac{kp\left(\frac{x}{c}\right)^{p-1}}{c\left[1+\left(\frac{x}{c}\right)^p\right]^{k+1}}$	$1-\left[1+\left(\frac{x}{c}\right)^p\right]^{-k}$	Brano et al. [13] Mazzeo et al. [31] Qin et al. [37]
D	$\frac{kp\left(\frac{x}{c}\right)^{kp-1}}{c\left[1+\left(\frac{x}{c}\right)^p\right]^{k+1}}$	$\left[1+\left(\frac{x}{c}\right)^{-p}\right]^{-k}$	Chiodo and Falco [38] Jung et al. [39] Jung and Schindler [14]
EGL	$\frac{k^2pc(1+xc)^{2p-1}e^{k-k(1+xc)^p}}{k+1}$	$1-\frac{e^{k-k(1+xc)^p}\left[1+k(1+xc)^p\right]}{k+1}$	Kantar et al. [10]
GG	$\lvert p\rvert\ x^{kp-1}\frac{e^{\left(-\frac{x}{c}\right)^p}}{c^{kp}\Gamma(k)}$	$\gamma_l\left(k,\left(\frac{x}{c}\right)^p\right)$	Morgan et al. [40] Kiss and Jnosi [35] Carta et al. [16]

that distinguish the MOA from a simple scan of all possible solutions to the problem. The MOA cleverly combines several concepts and simulates learning strategies to find the optimal solution efficiently and in a shorter period of time [50].

In MOA, the searching process for the optimal solution occurs through the minimization (or maximization) of an objective function, which is a previously defined function that is capable of numerically representing the quality of the generated solutions. In this study, three objective functions were used:

1. Maximization of the Coefficient of Determination (R^2): This widely used statistical test measures the correlation between the probabilities observed and the probabilities predicted by the distribution model, and it is given by [11]:

$$R^2=\frac{\sum_{i=1}^{n}\left(\widehat{F}_i-\overline{F}\right)^2}{\sum_{i=1}^{n}\left(\widehat{F}_i-\overline{F}\right)^2+\sum_{i=1}^{n}\left(F_i-\widehat{F}_i\right)^2} \tag{2}$$

where $\widehat{F}_i$ are the predicted cumulative probabilities obtained from cumulative distribution functions, F_i are the observed cumulative probabilities and $\overline{F} = \sum_{i=1}^{n} \widehat{F}_i/n$. The value of R^2 ranges from 0 to 1, with values close to 1 indicating a good fit. This objective function can also be interpreted as the minimization of the value $1 - R^2$ and was used by Jiang et al. [19] and Wang et al. [23].

2. Minimization of the Root Mean Square Error (*RMSE*): The RMSE is a measure of the accuracy of the fitted model and it is given by [5]:

$$RMSE = \sqrt{\frac{1}{n}\sum_{i=1}^{n}(F_i - \widehat{F}_i)^2} \tag{3}$$

The lower the *RMSE* value, the more accurate the fit. The minimization of the sum of squared errors as an objective function, which is very similar to the minimization of the *RMSE*, was used by Wang et al. [4] and Andrade et al. [25].

3. Minimization of $(1 - R^2) + NRMSE$: This is a hybrid objective function formed by the sum of the two previous functions. The term *NRMSE* means that the *RMSE* was normalized according to Eq. (4), so that R^2 and *RMSE* are in the same scale.

$$NRMSE = \frac{RMSE}{max(F) - min(F)} \tag{4}$$

Studies using this objective function to determine the unknown parameters of wind speed distributions were not found in the literature.

It is important to emphasize that the results generated from the three objective functions are not necessarily the same. Moreover, no studies were found that compared the performance of these objective functions in determining the optimal parameters of wind speed distributions. Therefore, once the results were obtained, a statistical analysis was conducted to determine which function was most suitable for this study.

According to Yang [48], when there is no time limit for the optimization process, it is theoretically possible for a given method to find the global optimum. In this context, if a maximum value of iterations were adopted as a stopping criterion, then the processing time would be restricted and the best solution found by the methods could be a premature and poorly optimized solution. Therefore, to avoid this possibility, the stopping criterion adopted in this work was the method convergence; that is, when the best solution obtained no longer suffers significant variations, the algorithm ceases and returns this solution.

Finally, to evaluate the performance of the MOA, the Maximum Likelihood Estimation (MLE) was also used. This method is widely used by many authors and it generally provides significant results, as can be seen in the studies conducted by Kantar et al. [10], Mohammadi et al. [5], Rocha et al. [21], Morgan et al. [40] and Jung and Schindler [51]. For a large number of samples, MLE is more efficient than other numerical methods [11]. Chang [18] compared the perfomance of the numerical methods MM, GM, EM, MLE, MMLE and EPF in estimating the Weibull parameters. Among these methods, the MLE was the one which perfomed better. In the study conducted by Katinas et al. [52], the MLE was also one of the methods which performed better when estimating the unknown parameters of the Weibull distribution.

In MLE, the model fitting is performed by identifying the parameters that maximize the probability of obtaining the observed data [1]. This method involves iterative processes and the simultaneous solution of different equations, thus requiring the use of a numerical method to obtain the result. Several different methods are used in the literature, such as Newton–Raphson, quasi-Newton, Nelder-Mead, among others. The Nelder-Mead method was used in this work.

The MLE is characterized as a deterministic numerical method; that is, for the same input, the output is always the same. In contrast, the MOA, which have in their structure random processes, have different outputs for the same input, which makes each run of the algorithm unique. Hence, in practice, several runs are required to obtain a good result [53].

4.1. Migrating Birds Optimization (MBO)

Proposed by Duman et al. [54], the MBO is inspired by the V-flight formation of migrating birds, in which the bird positioned in the front region, called the leader, guides the flock on both lines of the formation. Through this formation, birds receive an aerodynamic benefit from the bird in front and spend less energy during flight, which is the reason why birds adopt the V-flight formation. In a group of 25 birds, for example, each bird achieves, by virtue of this aerodynamic benefit, a flight range approximately 70% greater than that of a single bird [55]. The leader, by occupying the first position of the formation, does not receive such benefit and, consequently, expends more energy. More detailed and illustrated information about this method can be found in the studies conducted by Makas and Yumusak [56], Duman et al. [54] and Lissaman and Shollenberger [55].

The MBO simulates the benefit of energy saving by sharing solutions and is conducted as follows [56]:

1. Initialization and random distribution of the population of N_{birds} birds (solutions) in a V formation.
2. Generation of n_{nb} neighboring solutions for the leading bird. If one of these new solutions is better, then it replaces the leader. The $2n_{un}$ unused solutions are shared by the next two birds in the formation.
3. Generation of $n_{nb} - n_{un}$ neighboring solutions for each bird and then combining the solutions with the n_{un} solutions received from the birds in the front, totaling n_{nb} neighbors. If the neighboring solution is better, then it replaces the bird and the n_{un} unused solutions are shared with the next bird.
4. Step 3 is executed until all birds are processed.
5. In this step, it is assumed that the leader bird, after m iterations, reaches exhaustion. The leader is then shifted to the end of one of the two lines in the V formation and the second bird of this line takes the leader position.
6. Steps 2 to 5 are repeated until the stopping criterion is reached. The best solution obtained is returned.

In this algorithm, the neighboring solutions are generated according to Eq. (5), where b_{ij} is the ith solution consisting of j dimensions, being each dimension one of the parameters of the distribution models, $\widehat{b}_{ij}$ are the neighboring solutions, $r \in [1, N_{birds}]$ is an integer number other than i randomly chosen and $n_{[-1,1]}$ is a random number ranging from −1 to 1.

$$\widehat{b}_{ij} = b_{ij} + n_{[-1,1]}\cdot(b_{ij} - b_{rj}) \tag{5}$$

The leader bird spends the most energy by generating n_{nb} neighbors in each iteration. The other birds receive the n_{un} unused solutions from the birds in front and generate only $n_{nb} - n_{un}$ neighboring solutions, simulating the energy saving provided by the V-formation.

4.2. Imperialist Competitive Algorithm (ICA)

The ICA was proposed by Atashpax-Gargari and Lucas [57], and is an optimization method based on the sociopolitical process of imperialist competition. In this method, each country is a possible solution for the problem and the strongest countries are those with the best value of the objective function, also called cost in this algorithm. The ICA is conducted as follows [57]:

1. Random generation of the initial population of $N_{countries}$ countries. For the formation of empires, the N_{imp} countries with the lowest cost (best objective function value) are designated as imperialists, and the N_{col} remaining countries (called colonies) are distributed among the imperialists. The amount of colonies that each imperialist

receives is proportional to their power.
2. Movement of the colonies towards their respective imperialists (Assimilation) or in a random direction (Revolution). If one of the colonies become more powerful (better objective function value), then this colony becomes the imperialist of its respective empire.
3. Calculation of the total cost of all empires.
4. The weakest colony of the weakest empire is disputed among the strongest empires, so that the strongest empire is most likely to possess the weakest colony.
5. Elimination of the weaker empires. In this work, the elimination occurs when an empire has no colony.
6. Steps 2 to 5 are repeated until only one empire remains, being the last imperialist in the problem solution.

In the third step, the total cost TC_i of the ith empire is given by Eq. (6).

$$TC_i = Cost(imperialist_i) + (0.1)\cdot mean\{Cost(colonies\ of\ empire_i)\} \tag{6}$$

In the fourth step, the possession probability P_{p_i} of each empire is calculated by Eqs. (7) and (8), where NTC_i is the normalized total cost of the ith empire.

$$NTC_i = TC_i - max(TC) \tag{7}$$

$$P_{p_i} = \left| \frac{NTC_i}{\sum_{n=1}^{N_{imp}} NTC_n} \right| \tag{8}$$

For each empire, a random number $n_{[0,1]}$ between 0 and 1 is generated. The empire with the highest value of $P_{p_i} - n_{[0,1]}$ receives the colony being disputed.

4.3. Harmony Search (HS)

Initially proposed by Geem et al. [58], the HS is based on the artificial process of searching for the best consonance of musical notes by a musical group [41]. This combination of notes is called harmony. The search takes place through the group experience or a random process of improvisation. The quality of the new harmony generated is determined through an aesthetic criterion. Similarly, the HS seeks to mimic this behavior by optimizing existing solutions and randomly generating new solutions, adopting the value of the objective function as the quality criterion of the solutions.

HS is conducted as follows [58]:

1. Harmony Memory (HM) initialization. HM consists of N_h randomly generated harmonies, each one of which is a possible solution. In this study, each musical note that composes a harmony is one of the parameters of the wind speed distributions.
2. Improvisation of new harmonies. If the new harmony is better than the worst harmony present in HM, then the worst one is replaced by the new one.
3. Step 2 is repeated until the stopping criterion is reached.

In the second step, the generation of each musical note that composes the new harmony is governed by the Harmony Memory Considering Rate (*HMCR*), Pitch Adjusting Rate (*PAR*), and Bandwidth (*bw*) parameters. The *HMCR* ranges from 0 to 1 and is defined as the probability of an existing value in HM being selected to generate the new note, while 1 − *HMCR* is the probability of the new note being randomly generated from the total set of possible solutions. If *HMCR* is close to 1, then the solution diversity will not be preserved (worst global search), while if *HMCR* is close to 0, then the diversity will be high [59]. This parameter is very important because if the notes that compose the optimal solution are not present in HM, then it would be impossible to obtain this solution.

Each component obtained by the memory consideration is then examined to decide whether or not it should be pitch adjusted. For this purpose, the *PAR* parameter, which ranges from 0 to 1, is introduced and is defined as the probability of the generated musical note being replaced by an element in its neighborhood within a range $[-bw, bw]$ [41]. The *PAR* and *bw* parameters are responsible for local search and prevent the algorithm from stagnating in local minimums.

4.4. Cuckoo Search (CS)

The CS was proposed by Yang and Deb [60] and is based on the parasitic behavior of some Cuckoo bird species in combination with Lévy's flight.

Cuckoos are parasitic birds that usually lay their eggs in other birds' nest [19]. After egg deposition, the host may identify the parasitic egg, and if this occurs, then the cuckoo's egg is removed or the host leaves the nest and builds a new one elsewhere. Some cuckoo species are even capable of mimicking the pattern and color of the host nest eggs, which reduces their chances of being detected [60].

In the CS algorithm, each egg in a nest represents a potential solution to the problem, and each cuckoo egg deposited is a new solution. In addition, the algorithm obeys three idealized rules [61]:

- Each cuckoo lays only one egg at a time. The nest in which this egg will be deposited is chosen randomly.
- The best nests with high quality eggs (best solutions) are kept for the next generation.
- The number of host nests is fixed, and the probability of a cuckoo egg being detected is p_d. If the parasitic egg is detected, then it is removed or the host leaves the nest to build a new one.

The new solution of the ith cuckoo is generated through Lévy's flight, according to Eq. (9), where α is a constant usually equal to 1, and $\oplus$ means entrywise multiplications [4].

$$new\ solution_i = current\ solution_i + \alpha \oplus Lévy(\lambda) \tag{9}$$

Lévy's flight is defined as a random walk whose length of random steps follows the Lévy distribution (Eq. (10)), and the direction of these steps follows a uniform distribution. Through this flight mechanism, the new solutions can present very different values from the current best solution, which intensifies the global search process and prevents the algorithm from stagnating in local minimums [62].

$$Lévy(\lambda) \sim \tau = t^{-\lambda}, \quad (1 < \lambda \leqslant 3) \tag{10}$$

CS is conducted as follows [19]:

1. Random generation of the initial population composed of N_{nests} nests.
2. Calculation of the objective function for each nest, the best solution is kept for the next generation.
3. Generation of new solutions through Lévy's flight (Eq. (9)). If the new solution is better than the previous one, then the old one is replaced by the new one, otherwise the old solution is kept.
4. Generation of a random $n_{[0,1]}$ number between 0 and 1 for each nest. If $n_{[0,1]} > p_d$, then the cuckoo's egg is discovered and the host leaves the nest to build a new one. The new nests are compared with the nests obtained in step 3, so that only the best ones are kept.
5. Steps 2 to 4 are repeated until the stopping criterion is reached. The best solution obtained is returned.

5. Multi-criteria analysis for distribution model selection

Several statistical tests can be used to select the distribution model that best fits a region's wind speed data, such as: Root Mean Square Error [63], Relative Root Mean Square Error, Mean Absolute Error [32], Index of Agreement [4], Akaike Information Criterion [64], Bayesian Information Criterion [5], Kolmogorov–Smirnov Test [20], Power Density Error [1] and Coefficient of Determination [22,52].

However, when conducting an analysis with different criteria, the results may vary significantly between models and the analysis may be inconclusive [8]. Moreover, according to Kantar et al. [10], there is currently no consensus on which criterion is best for determining the most accurate distribution model. In a two-criteria analysis, for example, it is possible for one model to be the best in one criterion, and another model to be the best in another criterion. This would cause confusion and, consequently, a poor selection of the most accurate model. Amid this scenario, Masseran [8] proposed a multi-criterion approach based on multiplicative aggregation with a standardized score for each statistic criterion. In this process, all criteria are simultaneously considered and a single result is generated, which is adopted to select the most accurate model.

In the first step of this approach, the Kolmogorov–Smirnov Test (*KS*), Akaike Information Criterion (*AIC*), Deviation of Skewness and Kurtosis (*DSK*), and $1 - R^2$ statistical tests are calculated:

- *KS*: This test computes the largest difference between the predicted and the observed distribution and it is given by Eq. (11) [65]:

$$KS = max_{1 \leqslant i \leqslant n} |F_i - \widehat{F}_i| \tag{11}$$

where $\widehat{F}_i$ are the predicted cumulative probabilities from the fitted model and F_i are the observed cumulative probabilities of the wind speed data. A smaller *KS* indicates better fitting performance, and vice versa.

- *AIC*: This statistical test is a measure of information lost when a model is fitted to a dataset and is given by the Eq. (12), where L is the Likelihood function and n_p is the number of parameters of the fitted model [8]. The lower the *AIC*, the better the fit [33].

$$AIC = -2log(L) + 2n_p \tag{12}$$

- *DSK*: This is used to measure the similarity between the shape characteristics of the fitted model and the empirical distribution of data [8]. The skewness γ_1 and the kurtosis γ_2 of a distribution can be calculated, respectively, through Eqs. (13) and (14):

$$\gamma_1 = \frac{E(X^3) - 3E(X^2)E(X) + 2E^3(X)}{[\sqrt{E(X^2) - E^2(X)}]^3} \tag{13}$$

$$\gamma_2 = \frac{E(X^4) - 4E(X^3)E(X) + 6E(X^2)E^2(X) - 3E^4(X)}{[\sqrt{E(X^2) - E^2(X)}]^4} \tag{14}$$

where $E(X^n) = \int_0^\infty x^n f(x)dx$. The empirical skewness g_1 and the empirical kurtosis g_2 of the data are given, respectively, by the Eqs. (15) and (16), where $\bar{x}$ and s are, respectively, the average and the standard deviation of the wind speed data [14].

$$g_1 = \frac{\sum_{i=1}^{n} (x_i - \bar{x})^3}{(n - 1)s^3} \tag{15}$$

$$g_2 = \frac{\sum_{i=1}^{n} (x_i - \bar{x})^4}{(n - 1)s^4} \tag{16}$$

The *DSK* criterion is the calculated by Eq. (17). The smaller the *DSK*, the better the distribution fits the observed data [66].

$$DSK = \sqrt{(\gamma_1 - g_1)^2 \cdot (\gamma_2 - g_2)^2} \tag{17}$$

- $1 - R^2$: The R^2 test was presented earlier and is calculated by Eq. (2). Because the best possible value of R^2 is 1, the integrated approach uses the value $1 - R^2$, that way, the minimization of all criteria becomes indicative of a good fit.

Subsequently, each criterion is subjected to a standardization process in which a dataset with a given mean and standard deviation is converted into a dataset with mean 0 and standard deviation 1, according to Eq. (18):

$$z_{ij} = \frac{w_{ij} - \bar{w}_j}{s_j} \tag{18}$$

where w_{ij} is the ith value of the j criterion, z_{ij} is the standardized score, $\bar{w}_j$ and s_j are, respectively, the mean and standard deviation of the j criterion.

During standardization, it is possible that z-scores show positive and negative signs, which would affect the multiplicative aggregation. Therefore, to ensure that the standardized scores are comparable, the Standard Normal Cumulative Distribution Function Transformation (SNCDFT), given by Eq. (19), is used so that the values of z-scores are between 0 and 1.

$$\Phi(z_{ij}) = \frac{1}{\sqrt{2\pi}} \int_{-\infty}^{z_{ij}} e^{\frac{-t^2}{2}} dt \tag{19}$$

The z-scores of each criterion, after being submitted to SNCDFT, are multiplied and a single value is generated. In this work, this value is called Global Score (*GS*). The distribution with the lowest *GS* is the most suitable for the region and, as shown by Masseran [8], the model with the lowest *GS* presents not only the best fit in numerical terms but also the best fit graphically. Therefore, the use of this approach simplifies the comparative analysis between different models and ensures the objective selection of the most suitable distribution for a given region.

6. Results and discussion

6.1. Objective function selection

The results obtained through the three objective functions were compared for each probability distribution. Considering both regions analyzed, the maximization of the R^2 was the objective function that, in 55.68% of the cases, presented the lowest *GS*; that is, the best fit. The minimization of the *RMSE* and the Hybrid objective functions only ensured the best result in 25.00% and 19.32% of the cases, respectively. Therefore, the following discussion is based only on the results generated trough the maximization of the R^2. However, it is important to emphasize that, in this particular analysis, based on the *AIC*, *KS*, *DSK*, and $1 - R^2$ criteria, the objective function R^2 ensured good results. If an analysis is conducted with other statistical criteria, then the other two functions presented may provide better performance.

6.2. Station SCR-25

Once the distribution parameters were estimated, the $1 - R^2$, *KS*, *AIC* and *DSK* statistical tests for SCR-25 station were calculated and the results are presented in Table 4, including the Global Score *GS* generated from these four tests. In this section, we used the nomenclature $\text{Distribution}_{\text{Method}}$ to refer to a particular distribution model and to the method used to estimate its parameters; for example, GG_{ICA} refers to the GG distribution with parameters estimated by the ICA method.

By comparing, for example, the results of EGL_{MBO} and EGL_{HS}, the variation observed in the statistical tests would make it impossible to objectively decide which method ensured greater accuracy in parameter estimation. The result obtained through MBO is better in the $1 - R^2$ and *KS* tests, while the result obtained by the HS is better in the

Table 4
Results of the Coefficient of Determination ($1-R^2$), Kolgomorov-Smirnov Test (*KS*), Akaike Information Criterion (*AIC*) and Deviation of Skewness and Kurtosis (*DSK*) tests and the Global Score (*GS*) generated from the four tests in SCR-25.

Method	Model	$1-R^2$	*KS*	*AIC*	*DSK*	*GS*
MBO	W	0.000574	0.014455	238132.745	0.114126	0.009369
	G	0.003784	0.036525	244618.814	1.474199	0.051648
	BS	0.011968	0.071369	307993.008	3.753875	0.382511
	N	0.000786	0.020145	238968.175	0.251003	0.013540
	LN	0.009629	0.053931	266166.376	9.133399	0.390851
	GL	0.005056	0.043610	245272.189	2.643198	0.083748
	GEV	0.000253	0.011110	237936.878	0.022947	0.007442
	B	0.000534	0.017753	238491.024	0.217354	0.011528
	D	0.001943	0.022985	238187.991	0.096140	0.014818
	EGL	**0.000397**	**0.009580**	**237020.772**	**0.006519**	**0.006453**
	GG	0.000102	0.007636	237246.008	0.025975	0.005795
ICA	W	0.000357	0.015399	238130.005	0.128029	0.009732
	G	0.003900	0.035331	244982.699	1.401672	0.050449
	BS	0.009624	0.057409	295427.995	4.705488	0.356582
	N	0.000790	0.020240	238976.293	0.250689	0.013605
	LN	0.009568	0.053470	266863.515	8.798650	0.387863
	GL	0.005062	0.043675	245335.853	2.640323	0.084100
	GEV	0.000251	0.011352	237948.057	0.025259	0.007549
	B	0.000596	0.018732	238528.885	0.217207	0.012126
	D	**0.000796**	**0.018286**	**238520.273**	**1.607747**	**0.016699**
	EGL	0.000385	0.012710	237163.310	0.020883	0.007745
	GG	0.000190	0.007468	237251.611	0.023672	0.005766
HS	W	0.000353	0.014897	238114.779	0.126053	0.009477
	G	0.003787	0.035550	244719.734	1.452952	0.050359
	BS	0.009632	0.057295	295447.595	4.686767	0.355545
	N	0.000786	0.020224	238962.676	0.251681	0.013585
	LN	0.009594	0.054127	266735.745	8.921705	0.392168
	GL	0.005060	0.043604	245332.193	2.640350	0.083958
	GEV	0.000260	0.011895	237880.164	0.009455	0.007708
	B	0.000534	0.017413	238480.578	0.214431	0.011331
	D	0.002234	0.022562	238126.034	0.064479	0.014609
	EGL	**0.000433**	**0.010752**	**237003.080**	**0.004846**	**0.006889**
	GG	0.000102	0.007646	237249.452	0.026446	0.005800
CS	W	0.000353	0.014789	238112.183	0.125258	0.009423
	G	0.003783	0.036121	244660.830	1.465260	0.051108
	BS	0.009620	0.056998	296556.512	4.730798	0.356122
	N	**0.000786**	**0.020075**	**238964.664**	**0.251052**	**0.013496**
	LN	0.009563	0.053921	267044.953	8.726596	0.390115
	GL	0.005056	0.043399	245303.450	2.641275	0.083494
	GEV	0.000245	0.011140	237918.596	0.016894	0.007429
	B	0.000536	0.018090	238501.912	0.218988	0.011722
	D	0.000658	0.021876	238830.136	3.266149	0.026639
	EGL	0.000209	0.010214	237121.839	0.042366	0.006725
	GG	0.000103	0.007831	237252.272	0.026292	0.005865
MLE	W	0.001317	0.018823	238020.523	0.113605	0.011925
	G	0.015054	0.053450	243627.468	1.801609	0.112394
	BS	0.124033	0.146974	272893.147	10.994830	0.918208
	N	0.004060	0.028407	238798.948	0.263907	0.021988
	LN	0.051467	0.090703	258070.094	25.183177	0.733778
	GL	0.016834	0.054603	243740.888	2.829225	0.145563
	GEV	0.001244	0.017380	237592.360	0.000116	0.010478
	B	0.001796	0.021748	238526.282	0.232945	0.014821
	D	**0.002926**	**0.028497**	**238099.968**	**0.101334**	**0.019059**
	EGL	0.000821	0.014641	236949.896	0.005532	0.008597
	GG	0.000517	0.011197	236940.846	0.001241	0.007054

AIC and *DSK* tests. In this situation, it would be necessary to measure the importance of each criteria and the decision of the best model would be subjective. However, through the integrated approach, the analysis becomes more objective and more accurate. In this case, the *GS* of EGL_{HS} and EGL_{MBO} distributions are, respectively, 0.006889 and 0.006453, while the latter is the best in comparison.

This approach is useful not only to compare results obtained from different methods but also to compare different distribution models. For example, when comparing the results of the D_{ICA} and N_{CS} distributions, the D_{ICA} distribution has lower values of *KS*and *AIC*and N_{CS} distribution has lower values of $1-R^2$ and *DSK*. When compared in terms of *GS*, it is evident the better performance of N_{CS} with $GS = 0.013496$, while D_{ICA} provided $GS = 0.016699$. These two situations reaffirm the advantage and justify the use of an integrated approach in this study.

Comparing the same distribution model, it can be seen that the *GS* values obtained by the MOA are significantly lower than those obtained by the deterministic method MLE. The distribution D_{CS} was the only one that did not provide a lower *GS* value when compared to D_{MLE}. However, the other three methods used achieved this feat, demonstrating the applicability and high performance of the MOA in determining the parameters of the two and three-parameter distributions. Moreover, it can be seen that, in most distributions, the *GS* values obtained by the MOA showed slight variations, which demonstrates that these methods obtained similar solutions. For example, the *GS* of GL_{MBO}, GL_{ICA}, GL_{HS} and GL_{CS} are 0.083748, 0.084100, 0.083958 and 0.083494, respectively.

For the same parameter estimation method, the *GS* obtained by GG is the smallest and that obtained by LN is the largest. In the case of MLE, the *GS* from BS distribution is the largest. Therefore, among the analyzed distributions, GG was the one that provided the best fit in this region, while LN and BS presented the worst fits.

6.2.1. Optimal distribution model selection for SCR-25

To determine the probability distribution and the estimation method that guaranteed the best fit to the wind speed data from São João do Cariri, the result with the lowest *GS* from each distribution was extracted from Table 4 and the results are presented in Table 5. This also showed the position of each distribution in the rank. The estimated parameters of the distributions presented in Table 5 are provided in Table 6.

The distribution that provided the best fit was the GG_{ICA}, followed by EGL_{MBO} and GEV_{CS}, in second and third place, respectively.

The W_{MBO} distribution, which is one of the most widely used due to its versatility and good fit in different regions, ranked fourth, which confirms that this distribution is not always the most suitable. However, among the two-parameter distributions, the W_{MBO} was the one with the lowest *GS*.

Of all 11 distributions, the BS_{HS} and the LN_{ICA} were the ones that presented the worst values of *GS*. In general, it can be inferred that, in São João do Cariri, the three-parameter distributions, which were fitted through MOA with the objective function R^2, provided a better fit in relation to the two-parameter distributions, which were fitted in the same way and occupied the highest positions in the rank. In addition, it is important to emphasize, once again, that none of the best results were provided by the MLE, which proves that the MOA-based models performed better than the traditional NM-based models.

Fig. 2 provides a graph of each of the models presented in Table 5. For better visualization, the two and three-parameter distributions are presented separately.

From Fig. 2, it is possible to see that, among the two-parameter models, the W_{MBO} and N_{CS} distributions presented the best fits. The G_{HS}, GL_{CS}, BS_{HS} and LN_{ICA} distributions were the ones that presented the worst fits. These results are perfectly in agreement with the numerical result obtained through the integrated approach because, among the two-parameter models, the W_{MBO} and N_{CS} distributions had the lowest *GS* and the G_{HS}, GL_{CS}, BS_{HS} and LN_{ICA} distributions the highest *GS*.

It is also important to emphasize that this results are not affected by the bin size or bin numbers because all the three objective functions adopted in this work (See Eqs. (2)–(4)) were applied as a function of the predicted cumulative probabilities obtained from the fitted model ($\widehat{F}_i$) and the observed cumulative probabilities (F_i) at each data point. The bin size and the bin numbers are not variables of the Eqs. (2)–(4). Regarding the MLE, the bin size and the bin numbers are also not variables of this method.

All of the three-parameter distributions showed similar graphic

Table 5
Best result (lower *GS*) of each distribution model in SCR-25 (Extracted from Table 4).

Method	Models	$1-R^2$	*KS*	*AIC*	*DSK*	*GS*	Rank
MBO	W	0.000574	0.014455	238132.745	0.114126	0.009369	4
HS	G	0.003787	0.035550	244719.734	1.452952	0.050359	8
HS	BS	0.009632	0.057295	295447.595	4.686767	0.355545	10
CS	N	0.000786	0.020075	238964.664	0.251052	0.013496	6
ICA	LN	0.009568	0.053470	266863.515	8.798650	0.387863	11
CS	GL	0.005056	0.043399	245303.450	2.641275	0.083494	9
CS	GEV	0.000245	0.011140	237918.596	0.016894	0.007429	3
HS	B	0.000534	0.017413	238480.578	0.214431	0.011331	5
HS	D	0.002234	0.022562	238126.034	0.064479	0.014609	7
MBO	EGL	0.000397	0.009580	237020.772	0.006519	0.006453	2
ICA	GG	0.000190	0.007468	237251.611	0.023672	0.005766	1

Table 6
Parameters *k* (Shape parameter), *c* (Scale parameter), *p* (Second shape parameter) and *u* (Location parameter) of best distribution models in SCR-25. These values are the ones obtained from the simulations whose statistical tests are presented in Table 5.

Method	Models	*k*	*c*	*p*	*u*
MBO	W	2.3707	6.0098	–	–
HS	G	4.4726	1.2148	–	–
HS	BS	0.4840	4.9628	–	–
CS	N	1.2834	34.3363	–	–
ICA	LN	0.4827	1.6025	–	–
CS	GL	3.6083	0.5520	–	–
CS	GEV	−0.2166	2.3377	–	4.3102
HS	B	22.5375	21.7607	2.3911	–
HS	D	0.1947	7.9079	8.6932	–
MBO	EGL	0.2017	0.1964	3.0506	–
ICA	GG	0.7071	6.9428	2.9727	–

performance, except for D_{HS}. The D_{HS} displayed maximum density value in the interval $5-6$ m/s, while the maximum density observed in the data is in the interval $4-5$ m/s. Moreover, it can also be seen that for velocities between $9-11$ m/s, this distribution presented lower density than the observed data. This poor performance of the D_{HS} distribution agrees with its *GS* value, which was the worst among the three parameter distributions. As for the other three-parameter models, due to their great similarity, it is necessary to consider the *GS* values to determine which one was the most accurate, which in that situation was the GG_{ICA} with $GS = 0.005766$.

Regarding the performance of the MOA, the results presented in Table 5 are not conclusive to affirm if any method is superior. No method presented significant predominance in relation to the others. In other words, different methods ensured the best result in different distributions. However, it is worthy of note that the MBO and ICA methods, which were used to fit the two and three-parameter distributions for the first time in this study, guaranteed good results for the W and EGL, and LN and GG distributions, respectively. The HS, which was used for the first time in three-parameter distributions, provided the best result in G, BS, B, and D distributions. The CS guaranteed the best result in N, GL, and GEV distributions.

6.3. Station PTR-11

The statistical test results for PTR-11 station are shown in Table 7.

From Table 7, it is possible to see the advantages of using the integrated approach when comparing the results. For example, W_{ICA} and GEV_{CS}. The result provided by the ICA has lower values of *AIC* and *DSK*, while the result obtained by the CS has lower values of $1-R^2$ and *KS*. Comparing them in terms of *GS*, GEV_{CS} showed $GS = 0.007910$ and W_{ICA} showed $GS = 0.007894$, the latter is the best of the two.

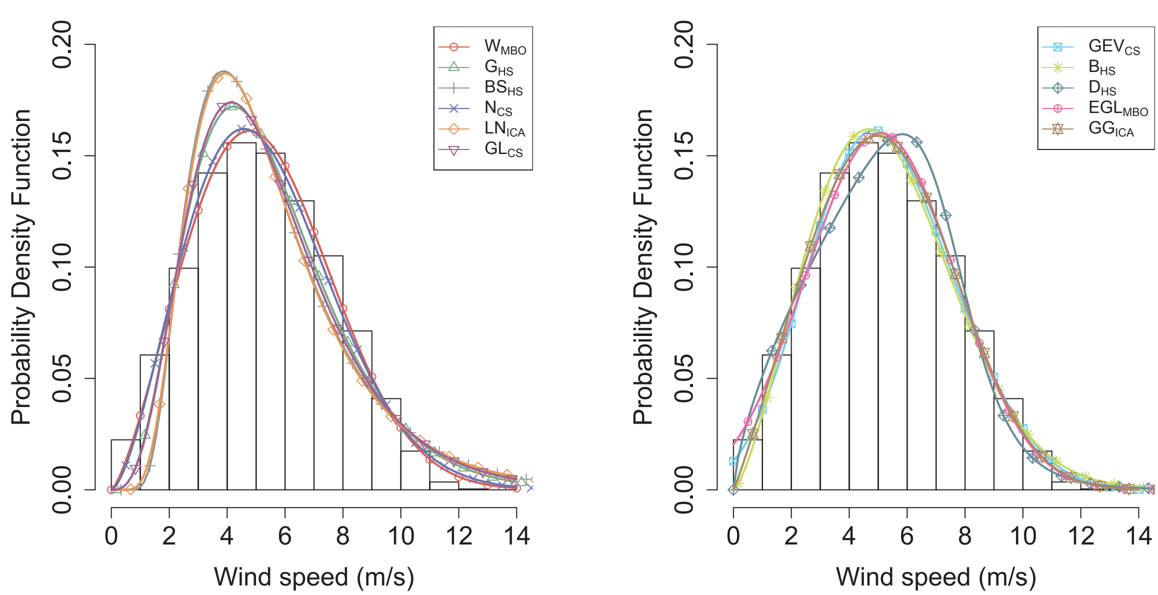

Fig. 2. Two (left) and three (right) parameters probability density functions in SCR-25. The curves obtained by the different probability density functions are plotted over the local histogram, to facilitate the performance comparison. The local histogram was built in 1 m/s bins, in accordance to the literature, and consequently the bin quantity was established by the wind speed range found in SCR-25. The 1 m/sk bins can be found, for example, in the studies conducted by Mohammadi et al. [5], Rocha et al. [21], Jiang et al. [19] and Usta and Kantar [64].

Table 7
Results of the Coefficient of Determination ($1 - R^2$), Kolgomorov-Smirnov Test (*KS*), Akaike Information Criterion (*AIC*) and Deviation of Skewness and Kurtosis (*DSK*) tests and the Global Score (*GS*) generated from the four tests in PTR-11.

Method	Model	$1-R^2$	*KS*	*AIC*	*DSK*	*GS*
MBO	W	0.000612	0.017412	209002.163	0.004601	0.008266
	G	0.004228	0.045361	218950.901	0.370237	0.051379
	BS	0.008148	0.062829	270459.619	1.550372	0.279593
	N	0.001783	0.031105	211471.356	0.018213	0.016877
	LN	0.008260	0.063264	243633.937	2.077473	0.300827
	GL	0.007615	0.055561	227299.561	1.966291	0.192398
	GEV	0.000576	0.014806	209148.212	0.055842	0.007755
	B	0.000624	0.018686	208870.487	0.019825	0.008748
	D	0.000310	0.012385	207765.650	0.177590	0.006860
	EGL	0.000426	0.009722	207496.629	0.011904	0.005246
	GG	0.000582	0.015121	208995.341	0.015806	0.007544
ICA	**W**	**0.000650**	**0.016483**	**208839.208**	**0.008137**	**0.007894**
	G	0.004259	0.047060	219403.763	0.357497	0.053866
	BS	0.008156	0.063038	270538.725	1.552027	0.280481
	N	0.001784	0.031222	211483.671	0.018225	0.016951
	LN	0.008031	0.061071	241838.032	2.233963	0.295729
	GL	0.007623	0.055233	227200.820	1.966589	0.190958
	GEV	0.000603	0.015276	209232.175	0.032188	0.007824
	B	0.000644	0.018596	208887.686	0.019816	0.008733
	D	0.000354	0.009717	207868.938	0.488103	0.007548
	EGL	0.000453	0.013724	207772.467	0.028113	0.006548
	GG	0.000624	0.013973	208932.538	0.023746	0.007194
HS	W	0.000613	0.017577	209029.892	0.004045	0.008336
	G	0.004453	0.050014	220256.394	0.337027	0.058689
	BS	0.008259	0.059861	267403.783	1.643141	0.278916
	N	0.001786	0.031230	211480.466	0.018219	0.016953
	LN	0.008323	0.056429	239133.621	2.484453	0.284167
	GL	0.007629	0.056887	227956.160	1.964457	0.199920
	GEV	0.000587	0.014901	209193.964	0.042432	0.007733
	B	0.000624	0.018845	208889.514	0.019486	0.008814
	D	0.000269	0.011278	207831.574	0.274764	0.007007
	EGL	0.000407	0.010054	207527.216	0.014464	0.005350
	GG	0.000591	0.015355	209062.035	0.026045	0.007721
CS	W	0.000612	0.017412	209002.166	0.004601	0.008266
	G	0.004228	0.045429	218966.785	0.369798	0.051473
	BS	0.008147	0.062742	270332.000	1.554897	0.279734
	N	0.001783	0.031104	211471.207	0.018213	0.016875
	LN	0.008027	0.061102	241806.339	2.239767	0.296050
	GL	0.007615	0.055575	227305.815	1.966273	0.192475
	GEV	**0.000573**	**0.015180**	**209203.073**	**0.055597**	**0.007910**
	B	0.000624	0.018747	208880.268	0.019537	0.008774
	D	0.000116	0.008508	207893.067	0.626664	0.007684
	EGL	0.000387	0.011380	207580.049	0.012057	0.005707
	GG	0.000582	0.015183	208992.895	0.015068	0.007559
MLE	W	0.003001	0.027339	208373.240	0.032883	0.012938
	G	0.025066	0.072438	215112.315	0.656764	0.125662
	BS	0.177518	0.175007	244775.917	6.572223	0.926383
	N	0.010131	0.048517	210121.376	0.012957	0.031527
	LN	0.063472	0.106895	227333.310	7.470845	0.663506
	GL	0.037652	0.083018	217336.642	2.112967	0.310026
	GEV	0.006277	0.036546	208778.585	0.023315	0.019597
	B	0.002752	0.026769	208423.086	0.037634	0.012663
	D	0.000655	0.015492	207675.236	0.145036	0.007761
	EGL	0.001231	0.017127	207336.423	0.006538	0.007471
	GG	0.003224	0.027008	208219.292	0.003414	0.012468

Comparing the same distribution model, it can be seen that all values of *GS* obtained by the MOA are significantly lower than those obtained by MLE, which again demonstrates the applicability and high performance of the MOA in determining the parameters of the wind speed distributions used. In addition, the *GS* values obtained by the MOA showed slight variations, which demonstrates that these methods obtained similar solutions. For example, the *GS* of N_{MBO}, N_{ICA}, N_{HS}, and N_{CS} are 0.016877, 0.016951, 0.016953 and 0.016875, respectively.

For the same parameter estimation method, the *GS* obtained by EGL is the smallest and that obtained by LN is the largest. In the case of MLE, the *GS* from BS distribution is the largest. Therefore, among the analyzed distributions, EGL provided the best fit in this region, while LN and BS presented the worst fits.

6.3.1. *Optimal Distribution Model Selection for PTR-11*

The result with the lowest *GS* from each distribution used in Petrolina was extracted from Table 7 and presented in Table 8. The estimated parameters of the best distribution models are provided in Table 9.

The distribution that provided the best fit was EGL_{MBO}, followed by D_{MBO} and GG_{ICA}, in second and third place, respectively.

The W_{ICA} distribution ranked fifth, confirming again that this distribution is not always the most suitable. However, among the two-parameter distributions, the W_{ICA} presented the lowest *GS*.

Of all 11 distributions, the BS_{HS} and the LN_{HS} had the worst values of *GS*. In general, it can be inferred that, in Petrolina, the three-parameter distributions, which were fitted through MOA with the objective function R^2, provided a better fit in relation to the two-parameter distributions, which were fitted in the same way and occupied the highest rank positions. Moreover, it is important to emphasize, once again, that none of the best results were provided by the MLE, which proves the good performance of the MOA.

Fig. 3 provides a graph of each model presented in Table 8. It is possible to see that from Fig. 3 that among the two-parameter models, the distribution W_{ICA} and N_{CS} presented the best fits. The W_{ICA} distribution was the one that best approximated the maximum density value observed in the histogram. Meanwhile, the distributions G_{MBO}, GL_{ICA}, BS_{HS} and LN_{HS} presented the worst fits. These results are perfectly in agreement with the *GS* values obtained because, among the two-parameter models, the W_{ICA} and N_{CS} distributions presented the lowest *GS* and the G_{MBO}, GL_{ICA}, BS_{HS} and LN_{HS} distributions had the highest *GS*.

All of the three-parameter distributions showed similar graphic performance, except for D_{MBO}. The D_{MBO} distribution displayed a maximum density value that was slightly higher than the maximum value observed in the histogram. However, it is possible to see subtle differences in this model in relation to the others. For example, in the $3-4$ m/s and $7-8$ m/s intervals, the density displayed by this distribution is slightly lower than the density obtained by the other three-parameter distributions. Thus, to avoid subjective conclusions in deciding the most accurate model, it is necessary to consider the values of the statistical tests. In this case, the EGL_{MBO} was the best with $GS = 0.005246$. The D_{MBO} model, which was the most distinct from the other three-parameter distributions, ranked second with $GS = 0.006860$.

Regarding the performance of the MOA, the results presented in Table 8 are not conclusive enough to affirm if any method is superior to the others. As in São João do Cariri, no method showed a significant predominance in relation to the others. The MBO and ICA methods ensured good results for the G, D and EGL, and W, GL, B and GG distributions, respectively. The HS method provided good results for the BS, LN and GEV models, and the CS for the N model.

7. Conclusion

Due to the lack of studies that apply optimization methods in the estimation of wind speed distribution parameters, four Metaheuristic Optimization Algorithms (MOA)—namely, Migrating Birds Optimization (MBO), Imperialist Competitive Algorithm (ICA), Harmony Search (HS) and Cuckoo Search (CS)—were used in this paper to determine the optimal parameters of 11 wind speed distribution models, which are mostly non-conventional models. This is the first time that MBO and ICA have been used for this purpose and is also the first time that HS has been applied to three-parameter distributions. Furthermore, to improve the accuracy in fitting the wind speed frequency, three objective functions were applied to the optimization

Table 8
Best result (lower *GS*) of each distribution model in PTR-11 (Extracted from Table 7).

Method	Models	$1-R^2$	*KS*	*AIC*	*DSK*	*GS*	Rank
ICA	W	0.000650	0.016483	208839.208	0.008137	0.007894	5
MBO	G	0.004228	0.045361	218950.901	0.370237	0.051379	8
HS	BS	0.008259	0.059861	267403.783	1.643141	0.278916	10
CS	N	0.001783	0.031104	211471.207	0.018213	0.016875	7
HS	LN	0.008323	0.056429	239133.621	2.484453	0.284167	11
ICA	GL	0.007623	0.055233	227200.820	1.966589	0.190958	9
HS	GEV	0.000587	0.014901	209193.964	0.042432	0.007733	4
ICA	B	0.000644	0.018596	208887.686	0.019816	0.008733	6
MBO	D	0.000310	0.012385	207765.650	0.177590	0.006860	2
MBO	EGL	0.000426	0.009722	207496.629	0.011904	0.005246	1
ICA	GG	0.000624	0.013973	208932.538	0.023746	0.007194	3

Table 9
Parameters *k* (Shape parameter), *c* (Scale parameter), *p* (Second shape parameter) and *u* (Location parameter) of best distribution models in PTR-11. These values are the ones obtained from the simulations whose statistical tests are presented in Table 8.

Method	Models	*k*	*c*	*p*	*u*
ICA	W	3.2446	5.4667	–	–
MBO	G	8.4757	0.5919	–	–
HS	BS	0.3521	4.7833	–	–
CS	N	2.2908	27.3741	–	–
HS	LN	0.3542	1.5636	–	–
ICA	GL	10.0910	0.8051	–	–
HS	GEV	−0.2891	1.6543	–	4.3059
ICA	B	23.2664	13.8914	3.3377	–
MBO	D	0.3000	6.3238	8.7330	–
MBO	EGL	0.0496	0.4040	3.2339	–
ICA	GG	0.8353	5.8091	3.6640	–

methods, and we subsequently identified which ensured greater accuracy. To evaluate the performance of the MOA, the deterministic method Maximum Likelihood Estimation (MLE) was used as a reference. Finally, our results were analyzed through an integrated approach that mutually considers four goodness-of-fit criteria that are commonly used in this type of study—namely, Coefficient of Determination (R^2), Kolgomorov-Smirnov Test (*KS*), Akaike Information Criterion (*AIC*) and Deviation of Skewness and Kurtosis (*DSK*)—in a single value, called a Global Score (*GS*). The present study was conducted in two cities of the Northeast of Brazil, which is one of the best regions in the world for wind power generation thanks to the extremely favorable characteristics of the wind regime.

When comparing the results obtained through the three objective functions, the maximization of the R^2 provided the best fit because the *GS* obtained through this objective function was the lowest in most of the distributions used.

When conducting the comparative analysis, the integrated approach proved to be extremely useful. Given the variations observed in the $1-R^2$, *KS*, *AIC*, and *DSK* statistical tests, it would be necessary to measure the importance of these tests to determine the most accurate distribution model. However, using the *GS* as a decision criterion, comparisons were made simply and objectively. In addition, the *GS* values perfectly matched the graphical performance of the fitted models because the best fitted models also had the lowest *GS* values.

In São João do Cariri, the wind speed distributions fitted through the MOA, except for the D_{CS} (Dagum distribution with parameters estimated by the CS method), showed higher accuracy when compared to the same distributions fitted by MLE; that is, the *GS* values obtained through the optimization methods were significantly lower than those obtained by the MLE. In Petrolina, every distribution fitted through the MOA presented higher accuracy. These results demonstrate the high

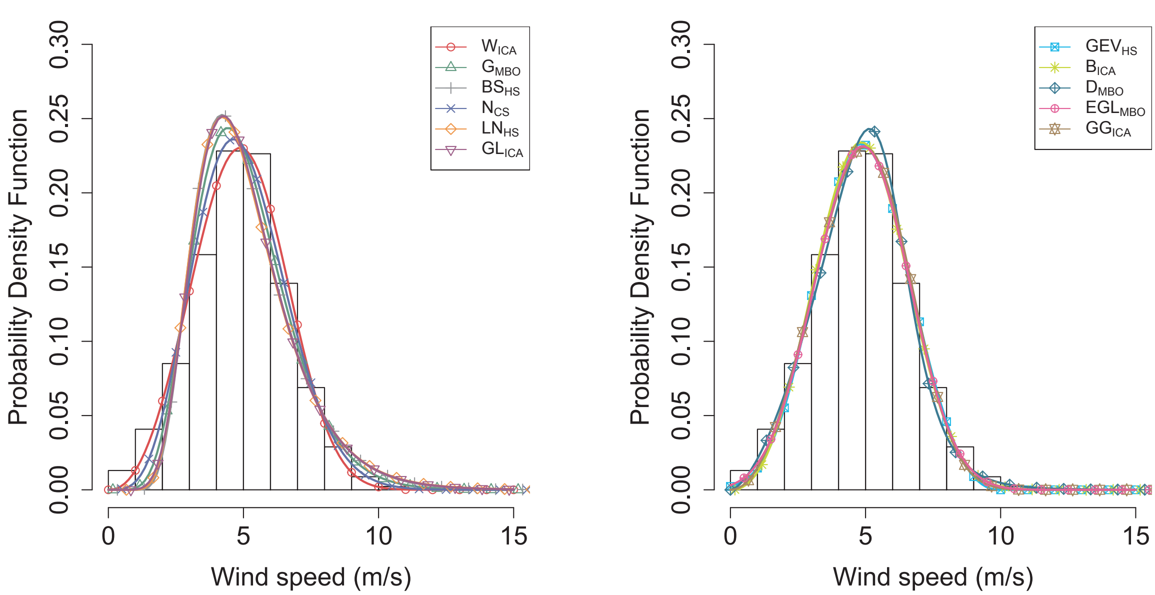

Fig. 3. Two (left) and three (right) parameters probability density functions in PTR-11. The curves obtained by the different probability density functions are plotted over the local histogram, to facilitate the performance comparison. The local histogram was built in 1 m/s bins, in accordance to the literature, and consequently the bin quantity was established by the wind speed range found in PTR-11. The 1 m/s bins can be found, for example, in the studies conducted by Mohammadi et al. [5], Rocha et al. [21], Jiang et al. [19] and Usta and Kantar [64].

performance of the MOA and their feasibility to determine the optimal parameters of two and three-parameter distributions. Regarding the performance of the MOA, the results were not conclusive enough to affirm if any one method is superior. Moreover, in both regions, the results obtained through the MOA were very similar because, for the same distribution, the four optimization methods provided close values of *GS*.

In both regions, the three-parameter models provided, in general, better fit (lower *GS*) than the two-parameter models. It was also shown that the widely used Weibull (W) distribution is not the most suitable. In São João do Cariri, the best fit was obtained through the GG_{ICA} (Gamma Generalized distribution with parameters estimated by the ICA method), which showed $GS = 0.005766$, and the W_{MBO} (Weibull distribution with parameters estimated by the MBO method) ranked fourth with $GS = 0.009369$. In Petrolina, the best fit was obtained through the recently proposed EGL_{MBO} (Extended Generalized Lindley distribution with parameters estimated by the MBO method) distribution, which showed $GS = 0.005246$, and the W_{ICA} (Weibull distribution with parameters estimated by the ICA method) distribution ranked fifth with $GS = 0.007894$. The Birnbaum-Saunders (BS) and Lognormal (LN) models presented the worst fits (highest *GS*) in both regions.

Data Availability

The raw wind speed data used in this study are openly available at:

- SCR-25: http://sonda.ccst.inpe.br/basedados/sjcariri.html
- PTR-11: http://sonda.ccst.inpe.br/basedados/petrolina.html

CRediT authorship contribution statement

Kevin S. Guedes: Conceptualization, Methodology, Conceptualization, Validation, Formal analysis, Investigation, Resources, Data curation, Writing - original draft, Writing - review & editing, Visualization, Supervision, Project administration, Funding acquisition. **Carla F. de Andrade:** Conceptualization, Validation, Formal analysis, Investigation, Resources, Visualization, Supervision, Project administration, Funding acquisition. **Paulo A.C. Rocha:** Conceptualization, Software, Validation, Formal analysis, Investigation, Resources, Writing - review & editing, Visualization, Supervision, Project administration, Funding acquisition. **Rivanilso dos S. Mangueira:** Validation, Investigation. **Elineudo P. de Moura:** Formal analysis, Investigation, Visualization.

Declaration of Competing Interest

The authors declare that they have no known competing financial interests or personal relationships that could have appeared to influence the work reported in this paper.

Acknowledgments

This study was financed in part by the Coordenação de Aperfeiçoamento de Pessoal de Nível Superior - Brasil (CAPES) - Finance Code 001 and accomplished with the support of the Conselho Nacional de Desenvolvimento Científico e Tecnológico - Brasil (CNPq), both Brazilian governmental agencies.

References

[1] Aries N, Boudia SM, Ounis H. Deep assessment of wind speed distribution models: A case study of four sites in Algeria. Energy Convers Manage 2018;155:78–90. ISSN 0196-8904.
[2] Akdag SA. Önder Güler, A novel energy pattern factor method for wind speed distribution parameter estimation. Energy Convers Manage 2015;106:1124–33. ISSN 0196-8904.
[3] Zhao X, Wang C, Su J, Wang J. Research and application based on the swarm intelligence algorithm and artificial intelligence for wind farm decision system. Renewable Energy 2019;134:681–97. ISSN 0960-1481.
[4] Wang J, Huang X, Li Q, Ma X. Comparison of seven methods for determining the optimal statistical distribution parameters: A case study of wind energy assessment in the large-scale wind farms of China. Energy 2018;164:432–48. ISSN 0360-5442.
[5] Mohammadi K, Alavi O, McGowan JG. Use of Birnbaum-Saunders distribution for estimating wind speed and wind power probability distributions: A review. Energy Convers Manage 2017;143:109–22. ISSN 0196-8904.
[6] Soukissian T. Use of multi-parameter distributions for offshore wind speed modeling: The Johnson SB distribution. Appl Energy 2013;111:982–1000. ISSN 0306-2619.
[7] Zhang H, Yu Y-J, Liu Z-Y. Study on the Maximum Entropy Principle applied to the annual wind speed probability distribution: A case study for observations of intertidal zone anemometer towers of Rudong in East China Sea. Appl Energy 2014;114:931–8. ISSN 0306-2619.
[8] Masseran N. Integrated approach for the determination of an accurate wind-speed distribution model. Energy Convers Manage 2018;173:56–64. ISSN 0196-8904.
[9] Wang J, Hu J, Ma K. Wind speed probability distribution estimation and wind energy assessment. Renew Sustain Energy Rev 2016;60:881–99. ISSN 1364-0321.
[10] Kantar YM, Usta I, Arik I, Yenilmez I. Wind speed analysis using the Extended Generalized Lindley Distribution. Renewable Energy 2018;118:1024–30. ISSN 0960-1481.
[11] Alavi O, Mohammadi K, Mostafaeipour A. Evaluating the suitability of wind speed probability distribution models: A case of study of east and southeast parts of Iran. Energy Convers Manage 2016;119:101–8. ISSN 0196-8904.
[12] Arslan T, Acitas S, Senoglu B. Generalized Lindley and Power Lindley distributions for modeling the wind speed data. Energy Convers Manage 2017;152:300–11. ISSN 0196-8904.
[13] Brano VL, Orioli A, Ciulla G, Culotta S. Quality of wind speed fitting distributions for the urban area of Palermo, Italy. Renewable Energy 2011;36(3):1026–39. ISSN 0960-1481.
[14] Jung C, Schindler D. Global comparison of the goodness-of-fit of wind speed distributions. Energy Convers Manage 2017;133:216–34. ISSN 0196-8904.
[15] Akdag SA, Dinler A. A new method to estimate Weibull parameters for wind energy applications. Energy Convers Manage 2009;50(7):1761–6. ISSN 0196-8904.
[16] Carta J, Ramírez P, Velázquez S. A review of wind speed probability distributions used in wind energy analysis: Case studies in the Canary Islands. Renew Sustain Energy Rev 2009;13(5):933–55. ISSN 0196-8904.
[17] Andrade CF, Neto HFM, Rocha PAC, Silva MEV. An efficiency comparison of numerical methods for determining Weibull parameters for wind energy applications: A new approach applied to the northeast region of Brazil. Energy Convers Manage 2014;86:801–8. ISSN 0196-8904.
[18] Chang TP. Performance comparison of six numerical methods in estimating Weibull parameters for wind energy application. Appl Energy 2011;88(1):272–82. ISSN 0306-2619.
[19] Jiang H, Wang J, Wu J, Geng W. Comparison of numerical methods and metaheuristic optimization algorithms for estimating parameters for wind energy potential assessment in low wind regions. Renew Sustain Energy Rev 2017;69:1199–217. ISSN 1364-0321.
[20] Kantar YM, Usta I. Analysis of the upper-truncated Weibull distribution for wind speed. Energy Convers Manage 2015;96:81–8. ISSN 0196-8904.
[21] Rocha PAC, Sousa RC, Andrade CF, Silva MEV. Comparison of seven numerical methods for determining Weibull parameters for wind energy generation in the northeast region of Brazil. Appl Energy 2012;89(1):395–400 ISSN 0306-2619, special issue on Thermal Energy Management in the Process Industries.
[22] Usta I, Arik I, Yenilmez I, Kantar YM. A new estimation approach based on moments for estimating Weibull parameters in wind power applications. Energy Convers Manage 2018;164:570–8. ISSN 0196-8904.
[23] Wang J, Qin S, Jin S, Wu J. Estimation methods review and analysis of offshore extreme wind speeds and wind energy resources. Renew Sustain Energy Rev 2015;42:26–42. ISSN 1364-0321.
[24] Wang Z, Wang C, Wu J. Wind energy potential assessment and forecasting research based on the data pre-processing technique and swarm intelligent optimization algorithms. Sustainability 2016;8:1191.
[25] Andrade CF, Santos LF, Macêdo MVS, Rocha PAC, Gomes FF. Four heuristic optimization algorithms applied to wind energy: determination of Weibull curve parameters for three Brazilian sites. Int J Energy Environ Eng 2019;10(1):1–12. ISSN 2251-6832.
[26] Chang TP. Wind energy assessment incorporating particle swarm optimization method. Energy Convers Manage 2011;52(3):1630–7. ISSN 0196-8904.
[27] Wu J, Wang J, Chi D. Wind energy potential assessment for the site of Inner Mongolia in China. Renew Sustain Energy Rev 2013;21:215–28. ISSN 1364-0321.
[28] ABEEólica. Associação Brasileira de Energia Eólica; 2019, http://abeeolica.org.br/, [accessed 2019-05-13], 2019.
[29] Garrido-Perez JM, Ordóñez C, Barriopedro D, García-Herrera R, Paredes D. Impact of weather regimes on wind power variability in western Europe. Appl Energy 2020;264:114731. ISSN 0306-2619.
[30] Sedaghat A, Hassanzadeh A, Jamali J, Mostafaeipour A, Chen W-H. Determination of rated wind speed for maximum annual energy production of variable speed wind turbines. Appl Energy 2017;205:781–9. ISSN 0306-2619.
[31] Mazzeo D, Oliveti G, Labonia E. Estimation of wind speed probability density function using a mixture of two truncated normal distributions. Renewable Energy 2018;115:1260–80. ISSN 0960-1481.
[32] Soukissian TH, Karathanasi FE. On the selection of bivariate parametric models for wind data. Appl Energy 2017;188:280–304. ISSN 0306-2619.
[33] Miao S, Gu Y, Li D, Li H. Determining suitable region wind speed probability

distribution using optimal score-radar map. Energy Convers Manage 2019;183:590–603. ISSN 0196-8904.
[34] Alavi O, Sedaghat A, Mostafaeipour A. Sensitivity analysis of different wind speed distribution models with actual and truncated wind data: A case study for Kerman, Iran. Energy Convers Manage 2016;120:51–61. ISSN 0196-8904.
[35] Kiss P, Jánosi IM. Comprehensive empirical analysis of ERA-40 surface wind speed distribution over Europe. Energy Convers Manage 2008;49(8):2142–51. ISSN 0196-8904.
[36] Ouarda T, Charron C, Shin J-Y, Marpu P, Al-Mandoos A, Al-Tamimi M, et al. Probability distributions of wind speed in the UAE. Energy Convers Manage 2015;93:414–34. ISSN 0196-8904.
[37] Qin Z, Li W, Xiong X. Estimating wind speed probability distribution using kernel density method. Electric Power Syst Res 2011;81(12):2139–46. ISSN 0378-7796.
[38] Chiodo E, Falco PD. Inverse Burr distribution for extreme wind speed prediction: Genesis, identification and estimation. Electric Power Syst Res 2016;141:549–61. ISSN 0378-7796.
[39] Jung C, Schindler D, Laible J, Buchholz A. Introducing a system of wind speed distributions for modeling properties of wind speed regimes around the world. Energy Convers Manage 2017;144:181–92. ISSN 0196-8904.
[40] Morgan EC, Lackner M, Vogel RM, Baise LG. Probability distributions for offshore wind speeds. Energy Convers Manage 2011;52(1):15–26. ISSN 0196-8904.
[41] Mansourzadeh F, Khamseh AG, Safdari J, Norouzi A. Utilization of harmony search algorithm to optimize a cascade for separating multicomponent mixtures. Progress Nucl Energy 2019;111:165–73. ISSN 0149-1970.
[42] Jaafari A, Zenner EK, Panahi M, Shahabi H. Hybrid artificial intelligence models based on a neuro-fuzzy system and metaheuristic optimization algorithms for spatial prediction of wildfire probability. Agric Forest Meteorol 2019;266–267:198–207. ISSN 0168-1923.
[43] Janardhanan MN, Li Z, Bocewicz G, Banaszak Z, Nielsen P. Metaheuristic algorithms for balancing robotic assembly lines with sequence-dependent robot setup times. Appl Math Model 2019;65:256–70. ISSN 0307-904X.
[44] Chiranjeevi K, Jena UR. Image compression based on vector quantization using cuckoo search optimization technique. Ain Shams Eng J 2018;9(4):1417–31. ISSN 0196-8904.
[45] Almeida FS. Optimization of laminated composite structures using harmony search algorithm. Comp Struct 2019;221:110852. ISSN 0263-8223.
[46] Gerist S, Maheri MR. Structural damage detection using imperialist competitive algorithm and damage function. Appl Soft Comput 2019;77:1–23. ISSN 1568-4946.
[47] Jalal M, Goharzay M. Cuckoo search algorithm for applied structural and design optimization: Float system for experimental setups. J Comput Des Eng 2019;6(2):159–72. ISSN 2288-4300.
[48] Yang X-S. Nature-inspired metaheuristic algorithms. Luniver Press; 2010.
[49] Shayanfar H, Gharehchopogh FS. Farmland fertility: A new metaheuristic algorithm for solving continuous optimization problems. Appl Soft Comput 2018;71:728–46. ISSN 1568-4946.
[50] Osman IH, Laporte G. Metaheuristics: A bibliography. Ann Oper Res 1996;63:513–628.
[51] Jung C, Schindler D. Wind speed distribution selection – A review of recent development and progress. Renew Sustain Energy Rev 2019;114:109290. ISSN 1364-0321.
[52] Katinas V, Gecevicius G, Marciukaitis M. An investigation of wind power density distribution at location with low and high wind speeds using statistical model. Appl Energy 2018;218:442–51. ISSN 0306-2619.
[53] Gomes WJ, Beck AT, Lopez RH, Miguel LF. A probabilistic metric for comparing metaheuristic optimization algorithms. Struct Saf 2018;70:59–70. ISSN 0167-4730.
[54] Duman E, Uysal M, Alkaya AF. Migrating Birds Optimization: A new metaheuristic approach and its performance on quadratic assignment problem. Inf Sci 2012;217:65–77. ISSN 0020-0255.
[55] Lissaman PBS, Shollenberger CA. Formation flight of birds. Science 1970(168):1003–5.
[56] Makas H, Yumusak N. System identification by using migrating birds optimization algorithm: a comparative performance analysis. Inf Sci 2016;24:1879–900.
[57] Atashpaz-Gargari EE, Lucas C. Imperialist competitive algorithm: an algorithm for optimization inspired by imperialistic competition. Proc IEEE Congress on Evol Comput 2007:4661–7.
[58] Geem ZW, Kim JH, Loganathan GA. New heuristic optimization algorithm: harmony search. Simulation 2001;76(2):60–8.
[59] Askarzadeh A, Zebarjadi M. Wind power modeling using harmony search with a novel parameter setting approach. J Wind Eng Ind Aerodynam 2014;135:70–5.
[60] Yang XS, Deb S. Cuckoo Search via Lévy Flights. In: Proceedings of world congress on nature & biologically inspired computing (NaBIC 2009); 2009, p. 210–14.
[61] Yang SDXS. Engineering optimisation by cuckoo search. Int J Mathe Modell Num Optim 2010;1(4):330–43.
[62] Emary E, Zawbaa HM, Sharawi M. Impact of Lévy flight on modern meta-heuristic optimizers. Appl Soft Comput 2019;75:775–89. ISSN 1568-4946.
[63] Akdag SA, Güler Önder. Alternative Moment Method for wind energy potential and turbine energy output estimation. Renewable Energy 2018;120:69–77. ISSN 0960-1481.
[64] Usta I, Kantar YM. Analysis of some flexible families of distributions for estimation of wind speed distributions. Appl Energy 2012;89(1):355–67 ISSN 0306-2619, special issue on Thermal Energy Management in the Process Industries.
[65] Ouarda T, Charron C, Chebana F. Review of criteria for the selection of probability distributions for wind speed data and introduction of the moment and L-moment ratio diagram methods, with a case study. Energy Convers Manage 2016;124:247–65. ISSN 0196-8904.
[66] Tofallis C. Selecting the best statistical distribution using multiple criteria. Comput Ind Eng 2008;54(3):690–4. ISSN 0360-8352.